Asian Journal of Chemistry; Vol. 34, No. 11 (2022), 2872-2878

ASIAN JOURNAL OF CHEMISTRY

https://doi.org/10.14233/ajchem.2022.23956

Improvement of Poly(L-lactide)-*b*-poly(ethylene glycol)-*b*-poly(L-lactide) Film Properties with Nanocellulose

CHUTIMA BANTHAO[1,2], YODTHONG BAIMARK[1,2], SUJITRA WONGKASEMJIT[3] and KANSIRI PAKKETHATI[1,2,*]

[1]Biodegradable Polymer Research Unit, Department of Chemistry, Faculty of Science, Mahasarakham University, Mahasarakham 44150, Thailand
[2]Center of Excellence for Innovation in Chemistry (PERCH-CIC), Faculty of Science, Mahasarakham University, Maha Sarakham 44150, Thailand
[3]Petroleum and Petrochemical College, Chulalongkorn University, Bangkok 10330, Thailand

*Corresponding author: E-mail: kansiri.p@msu.ac.th

Received: 8 June 2022; *Accepted*: 28 July 2022; *Published online*: 19 October 2022; AJC-20999

In present study, the improvement of poly(L-lactide)-*b*-poly(ethylene glycol)-*b*-poly(L-lactide) or PLLA-PEG-PLLA film properties with extract of rice straw nanocellulose are reported. The diameter of cellulose particles was 59.92 and 392 nm as determined by TEM and particle size analysis, respectively. A solvent casting method was used to prepare nanocellulose and polymer matrix (PLLA-PEG-PLLA) in different ratios (1%, 3% and 5% wt). It was found that the nanocellulose content, thermal and mechanical properties of the polymer matrix were varied. There was slightly increased thermal stability from 270 to 276 ºC in the first stages. In the 2nd stage from 367 to 376 ºC, TGA indicated slightly decreased T_g and T_{cc} while T_m was not different (DSC). The mechanical properties of biocomposite film displayed slightly increased Young's modulus (414-447 MPa), stress at break (26-31 MPa) and elongation at break (6.6-7.6%) compared to pure PLLA-PEG-PLLA film.

Keywords: Biodegradable polymer, Poly(L-lactide)-*b*-poly(ethylene glycol)-*b*-poly(L-lactide), Nanocellulose.

INTRODUCTION

Plastics are mostly produced from petroleum and are light weight, inexpensive and high strength. Plastics are generally non-biodegradable or might take centuries to decay the causing environmental problems. In last few decades, researchers around the world have been trying to create materials that replace petroleum based plastics. Biodegradable polymers can be divided into two types according to the source, which are natural resources such as starch, chitosan, *etc.* [1] and synthesis processes such as poly(lactic acid) (PLA), poly(glycolic acid) (PGA) and poly(caprolactone) (PCL), *etc*. [2]. Synthetic polymers are created from monomers, for instance glycolic acid (GA), lactic acid (LA) and ε-caprolactone (CL). Biodegradable polymers from synthesis are widely used in many biomedical applications such as implantable devices [3], drug delivery systems [4] and tissue engineering [5].

Polylactic acid (PLA) is an aliphatic polyester produced using lactic acid (2-hydroxy propionic acid) as a basic building block. It is a compostable thermoplastic and biodegradable and derived from renewable plant sources, such as starch or sugar. The processing of PLA can be achieved in many ways through conventional techniques such as extrusion, injection and spinning. The exceptional mechanical properties of PLA are dependent on the optical purity, molecular weight and degree of crystallinity. Generally, the PLA properties are similar to those of polystyrene [6]. The disadvantages are many and obvious for PLA *e.g*. its degradation rate is unresponsive to a wide range of application-specific requirements and there are no cell recognition sites that are important for tissue compatibility on the surface of PLA application in tissue engineering. On the other side, in the case of using PLA directly as a packaging material, brittle breakage has often occurred. Therefore, this property must be modified in PLA. Modifications of PLA include copolymerizing of the lactide with other lactone-type monomers, hydrophilic macro-initiators such as polyethylene glycol (PEG) or other monomers with functional groups (such as amino and carboxylic groups, *etc.*) and the blending PLA with other materials.

Poly(ethylene glycol) is highly biocompatible, soluble in aqueous solutions as well as in organic solvents, supports its excellent biocompatibility and processability, respectively. When PEG is combined with PLA results in the improved mechanical properties and hydrophilicity of PLA [4]. The low molecular weight PEG has been shown to have good miscibility with PLA matrices. However, it has fast migration from the matrices to surfaces on aging. However, high molecular weight PEG reduces the migration effect but phase separation of matrices [7].

Poly(L-lactide)-block-poly(ethylene glycol)-block-poly-(L-lactide) or PLLA-PEG-PLLA has been used extensively in drug delivery systems [4,6]. The expectional properties of PLLA-PEG-PLLA exhibited felxibility and high hydrophilicity compared with PLA due to the high chain mobility of hydrophilic PEG blocks [8]. Good phase compatibility [9] was also reported for PLLA-PEG-PLLA matrix but has low mechanical strength and therefore, is not suitable for some applications.

Rice straw is used for various things such as animal feed, making compost or use as a material for straw mushroom cultivation, however the rice straw is still in large amount as waste. For this reason, some farmers have eliminated rice straw by burning which results in environmental impacts. Nanocellulose is used to reinforce the polymer and improved mechanical properties such as pineapple leaves [10], banana fibers [11], wood flour [12], *Agave tequilana* weber waste [13] and grape residue [14]. Thus, nanocellulose has been extracted from rice straw to reduce environmental pollution and increase the value of rice straw. The properties of nanocellulose include low density [10], high strength [15] and high thermal property [16]. The biocomposite films between poly(L-lactide)-*b*-poly (ethylene glycol)-*b*-poly(L-lactide) and nanocellulose were developed to improve their mechanical and thermal properties.

EXPERIMENTAL

Nanocellulose was extracted from the rice straw (jasmine rice procured from the local village in Mahasarakham province, Thailand). Chemicals *viz*. NaOH (AR grade, Ajax Finechem), H_2O_2 (30-32%), H_2SO_4 (98%) and CH_2Cl_2 (AR grade, Fisher chemical) was used as solvent. Poly(L-lactide)-*b*-poly(ethylene glycol)-*b*-poly(L-lactide) or PLLA-PEG-PLLA, Mn = 89,900 g/mol) was supplied by Biodegradable Polymer Research Unit, Department of Chemistry, Mahasarakham University.

Extraction of nanocellulose from rice straw: The preparation of nanocellulose can be divided into two parts. In first part (extraction of cellulose), the rice straw was cut into small pieces, dirt was removed with tap water and then dried in an oven at 80 ºC. The rice straw was extracted with 2 M NaOH for the elimination of hemicellulose and then removed lignin using 18.5% H_2O_2. In second part, nanocellulose and cellulose fibers were hydrolyzed using 64% H_2SO_4 (v/v) (1 g/10 mL)) at 45 ºC for 0.5 h. According to a reported method [17,18] under constant stirring, cold water was added to stop the hydrolysis reaction. The suspension of cellulose was washed five times with distilled water by centrifugation (10,000 rpm, 4 ºC, 15 min) [18,19] to remove excess sulfuric acid and then dialyzed against distilled water using cellulose membranes with a molecular weight cut-off of 12-14 kDa [17] until a constant pH was achieved. It was thoroughly dispersed using a sonicator bath (at 45 ºC, 0.5 h) and was freeze-dried and then stored in a desiccator.

Fabrication biocomposite films: The PLLA-PEG-PLLA was dissolved in 15 mL dichloromethane (1 h) before mixing nanocellulose for 0.5 h with stirring. The suspension was poured onto a petri dish before drying at room temperature for 12 h. The obtained biocomposite films were prepared in a vacuum oven at room temperature for 24 h. The ratios of biocomposite films in this work were 1, 3 and 5% wt.

Characterization: The morphology and structure of nanocellulose were studied using a transmission electron microscope (FEI, Tecnai G2 20). For preparation, the nanocellulose (20 µL) was dropped on parafilm. Then, the formvar/carbon mesh grid 300 mesh dully side was placed on the nanocellulose for 5 min. The grid was wiped using a triangle filter paper, washed (2 drops of distilled water) and then 2% uranyl acetate added to the grid for 1 min. After that the grid was stored in a desiccator cabinet for 24 h and was analyzed by TEM at a potential of 200 KeV. A scanning electron microscope (SEM) (JEOL, JSM-64606V) was used to study the surface and morphology (shape, pattern, size) of the biocomposite films. For the cross-section study of the biocomposite films, the films were immersed in liquid nitrogen for 30 min and broke it to 2 pieces. Then, the biocomposite films were coated with gold for 15 min. The average particle size and size distribution of the nanocellulose were evaluated by a particle size analyzer (Malvern, Zetasizer Nano S9) in a water medium. In this study, the crystallinity of nanocellulose and biocomposite films was measured using an X-ray diffractometer (XRD) (Bruker D8, Advance) at room temperature using Cu$K\alpha$ radiation at 40 kV and 40 mA. For XRD, the scanning angle range of 2θ = 5-40º at a scan speed of rate 0.2º/s was used to determine the crystalline structures.

The thermal properties of biocomposite films were determined with a differential scanning calorimeter (DSC), (Perkin-Elmer, Pyris Diamond) under a nitrogen gas flow. The composite films (about 3-5 mg) were weighed and heated at 200 ºC for 2 min to remove their thermal history. For DSC thermograms, the biocomposite films were heated from -10 to 205 ºC at the rate of 10 ºC/min. For cooling DSC thermograms, the sample was held at 205 ºC for 1 min then cool to -10 ºC at the rate of 10 ºC/min. The thermal properties of biocomposite films were examined using a thermogravimetric analyzer (TA-Instrument, TG SDT Q600) and heated from 50 to 800 ºC at the rate of 20 ºC/min under a nitrogen gas atmosphere. The mechanical properties of the biocomposite films were examined on Universal testing machine (Dongguan Liyi Environmental Technology, LY-1066B) according to ASTM D882. The sizes of the biocomposite films were 1 cm × 8 cm having the gauge length 25 mm and crosshead speed 50 mm/min.

RESULTS AND DISCUSSION

Morphology studies: The fabrication of biocomposite film between nanocellulose and PLLA-PEG-PLLA was done by solvent casting method. It was found that the nanocellulose

was a white powder [20,21]. The SEM image (Fig. 1a) of cellulose after the hydrolysis process displayed small rod-like crystals. Transmission electron microscope (TEM) images (Fig. 1b) of nanocellulose displayed a nano-size dimensions with a diameter of 15-20 nm and a rod-like crystal structure, proving that cellulose fibers were isolated from rice straw at the nanometer scale. This result was consistent with Thakur *et al.* [19]. The nanocellulose agglutinated because of the drying (freeze drying), suspension process [19,22] or possibly due to the strong intermolecular hydrogen bond [23].

The SEM and TEM images of the prepared PLLA-PEG-PLLA/NC biocomposite films at different compositions showed an agglomeration (Fig. 2). The physical appearances of biocomposite films (1-5% wt.) were found to be slightly less transparent than pure PLLA-PEG-PLLA film.The results showed that the pure PLLA-PEG-PLLA film was smooth and uniform [7]. When nanocellulose was added, it was observed a phase separation of the uniform phase (nanocellulose phase) in the PLLA-PEG-PLLA matrix. The biocomposite films showed an agglomerate of nano-cellulose with increasing content of nanocellulose [11]. These agglomerated nanocellulose in the PLLA-PEG-PLLA matrix were observed as the nanocellulose content increased due to high hydrophilicity of nanocellulose.

Particle size: The analysis particle size of nanocellulose powder dispersed in water determined by particle size analyzer (Fig. 3) displayed a sharp peak at around 59.92 nm and 392 nm [24] diameter. The average particle size of nanocellulose displayed 2θ peaks which are larger particle sizes than reported in previous research [19]. This may be have been due to the drying process [22] of the nanocellulose having effects on their agglomeration [21,25].

FTIR studies: The main functional groups of pure nanocellulose, pure PLLA-PEG-PLLA film and PLLA-PEG-PLLA/NC biocomposite films were examined by ATR-FTIR (Fig. 4). The dominant function of nanocellulose, the broad and high intensity 3500-3000 cm^{-1} [17,26], 2900 cm^{-1} [17] correspond to the CH stretching region and at 950 cm^{-1} [19] was due to the C-O-C glycosidic ether. For pure PLLA-PEG-PLLA film, the dominant function was observed at 1750 cm^{-1} and at 1103 cm^{-1} and the presence of carboxylic ester (C=O), ether (C-O)

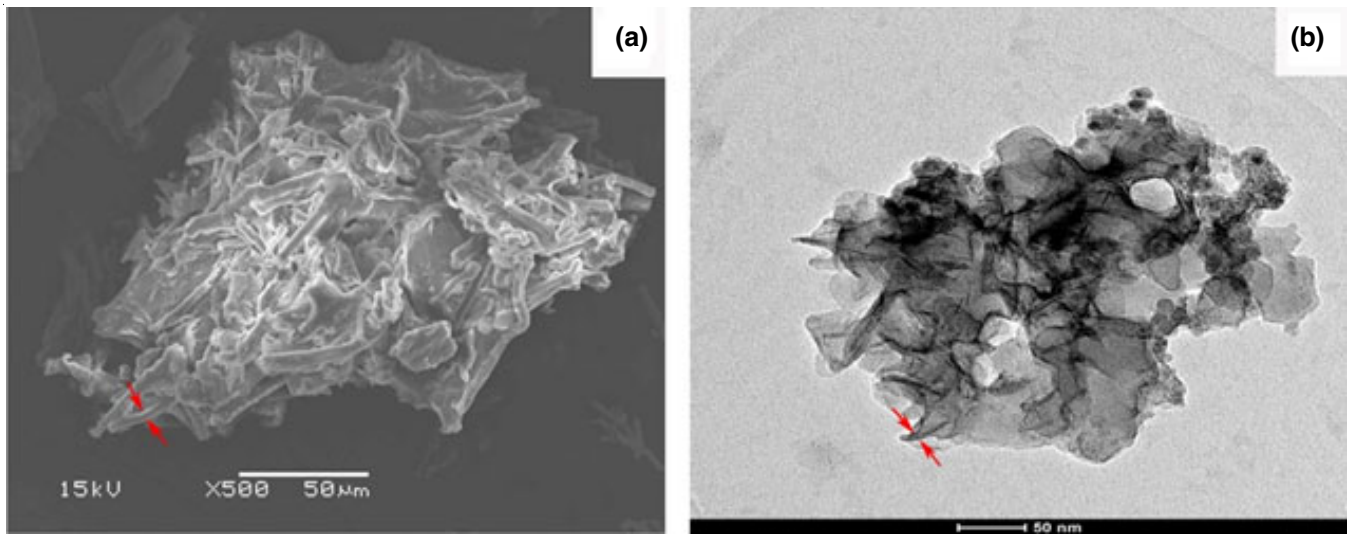

Fig. 1. (a) SEM images and (b) TEM images of nanocellulose

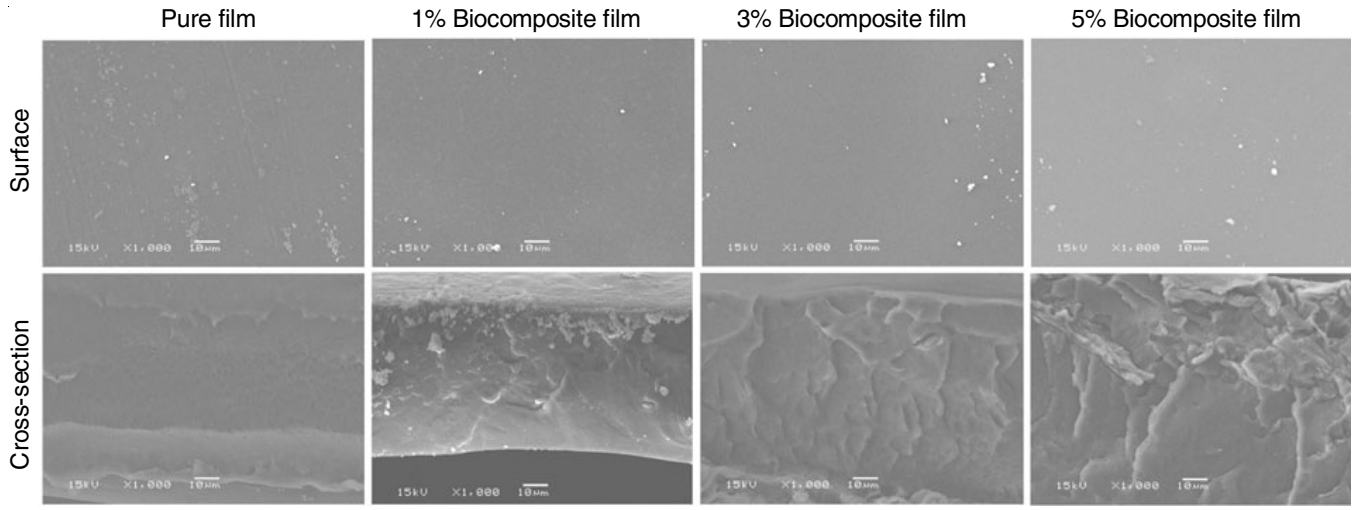

Fig. 2. SEM images of pure PLLA-PEG-PLLA film, PLLA-PEG-PLLA/NC biocomposite films with 210 µm thickness

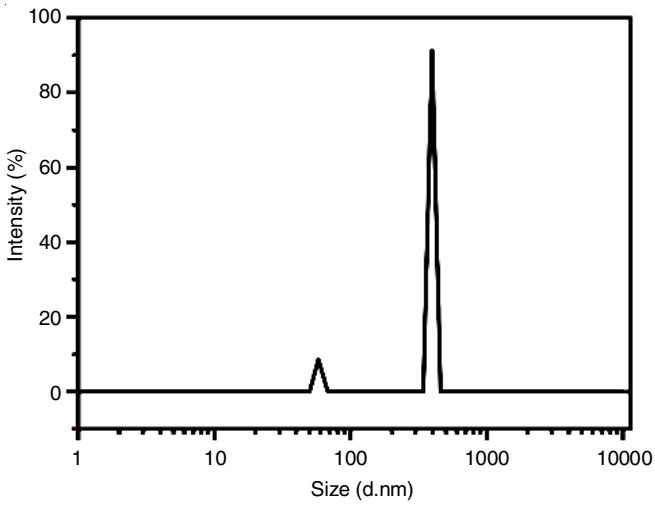

Fig. 3. Particle average size of nanocellulose

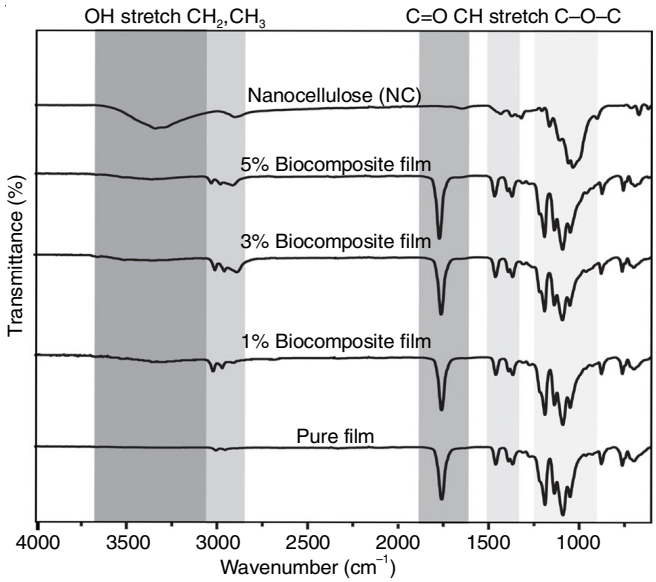

Fig. 4. ATR-FTIR analysis of pure PLLA-PEG-PLLA film, PLLA-PEG-PLLA/NC biocomposite films and pure nanocellulose

groups, the peak at 2800 cm^{-1} indicated the C-H stretching [27-29]. The influence of nanocellulose based on PLLA-PEG-PLLA or biocomposite films exhibited a broad-spectrum and high intensity of 3500-3000 cm^{-1} (OH *str.*), whereas a high shape peak at 1750 cm^{-1} is due to the carboxylic ester (C=O). The results of this study confirmed the presence of two components of nanocellulose and PLLA-PEG-PLLA. It was also found that the biocomposite films exhibited a more prominent OH function group with a higher nanocellulose content, possibly due to nanocellulose enclosed in a higher OH function group [23].

XRD studies: The XRD patterns of pure PLLA-PEG-PLLA film and PLLA-PEG-PLLA/NC are shown in Fig. 5, where the fabricated polymer having nanocellulose exhibited small and broad peaks at 2θ = 15.7º [20], 22.4º [17,19] and 34.4º [19]. The crystallinity index (Crl) using Segal's formula [30,31] of the fabricated nanocellulose was found to be 59.9%, which is in accord with the previous studies [17,20,21,32]. The characteristic high-intensity diffraction peak at 16.6º was

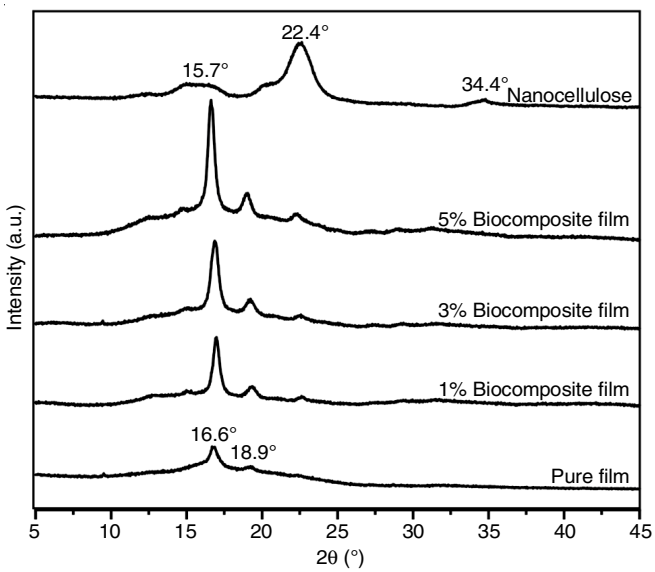

Fig. 5. XRD patterns of pure PLLA-PEG-PLLA film, PLLA-PEG-PLLA/NC biocomposite films and pure nanocellulose

attributed to the PLLA block, whereas the peak at 18.9º is attributed to the PEG block, revealed the natural crystalline form of PLLA-PEG-PLLA consistent [7,29,33]. When added the different ratios of nanocellulose to PLLA-PEG-PLLA biocomposite films, the peaks at 16.6º, 18.9º and 22.4º showed a higher intensity as nanocellulose likely to be acted as a nucleating agent [34,35].

Mechanical properties: The mechanical properties of pure PLLA-PEG-PLLA film and PLLA-PEG-PLLA/NC biocomposite films were measured using a tensile testing machine (Fig. 6). The Young's modulus, also known as elastic modulus, and stress at break are the two key indicators of a material's stiffness and ductility, respectively. In pure PLLA-PEG-PLLA film, the stress at break was 31.5 MPa, elongation at break (18.1%) and Young's modulus (509 MPa), which were consistent with the previous studies [7,33]. After the addition nanocellulose, the biocomposite films displayed a slightly increased Young's modulus (414-447 MPa), stress at break (26-31 MPa) and elongation at break (6.6-7.6%), which is due to the aggregation effect. The results showed that adding nanocellulose to the biocomposite film slightly decreased stress at break and Young's modulus. The nanocellulose showed the poor interfacial adhesion between the polymer matrix and the filler, which leads to the lower stress at break and Young's modulus [23]. However, an increase in stiffness of the film, on the other hand, decreased the elasticity as evident from the significant decrease in percent elongation at break of biocomposite films [11].

Thermal studies: The thermal stability patterns of the nanocellulose and PLLA-PEG-PLLA/NC biocomposite films are shown in Fig. 7. The thermal degradation of nanocellulose showed a multi-stage process following the different non-cellulosic and cellulosic components. The TGA of all samples exhibited a small initial mass loss around 100 ºC from the evaporation of adsorbed moisture, followed by the significant mass loss due to decomposition and mass loss from burning.

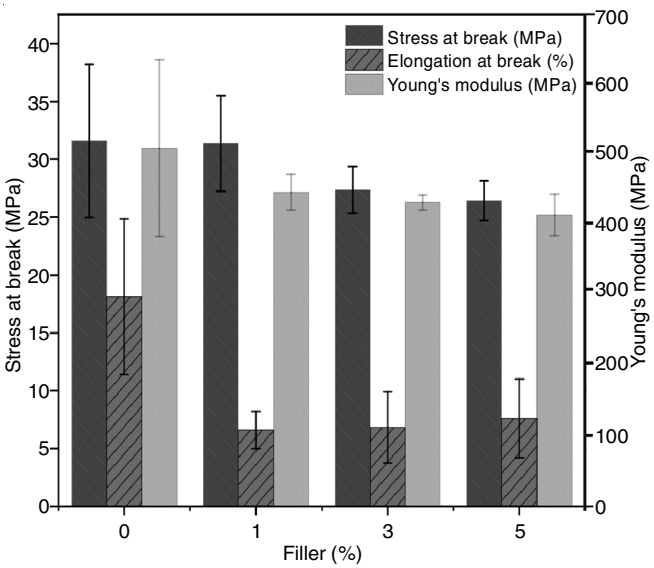

Fig. 6. Tensile properties of pure PLLA-PEG-PLLA film pure PLLA-PEG-PLLA film, PLLA-PEG-PLLA/NC biocomposite films and pure nanocellulose

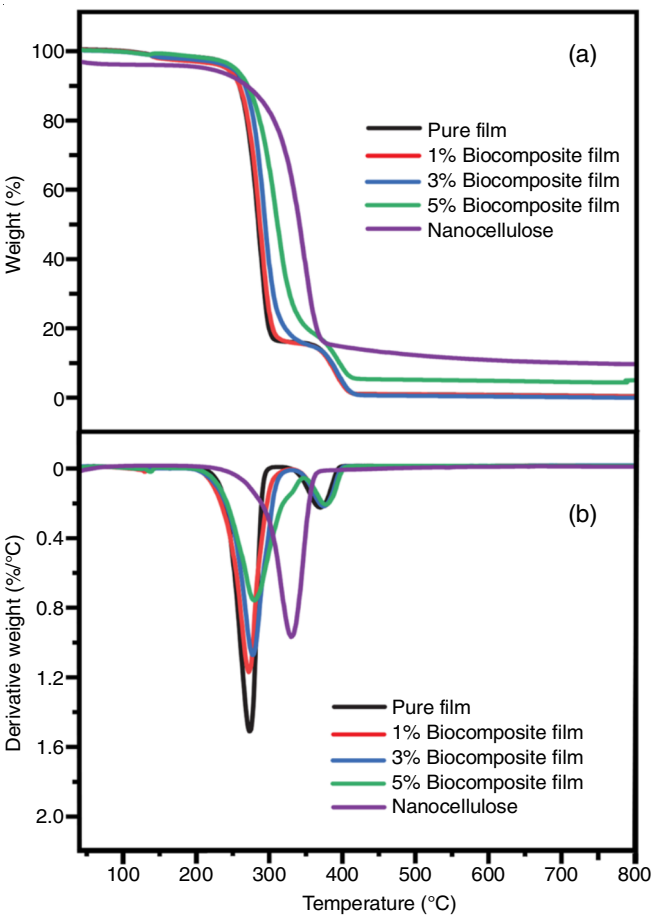

Fig. 7. TGA (a) and DTG(b) curves of pure PLLA-PEG-PLLA film pure PLLA-PEG-PLLA film, PLLA-PEG-PLLA/NC biocomposite films and pure nanocellulose

Another phase of degradation started at 250-290 ºC [17,23,36] which was happened due to the thermal depolymerization of hemicelluloses and the breakdown of glycosidic linkages of cellulose. The third phase of degradation was occured due to the decomposition of lignin at the temperature range of 250-420 ºC [19].

The pure PLLA-PEG-PLLA film displayed the two-step thermal decompositions of PLLA blocks and PEG blocks in the temperature ranges of 250-350 ºC and 350-450 ºC, respectively. The temperature value where the maximum weight loss occurred, as maximum decomposition rate (Td_{max}) are shown in Table-1. The Td_{max} and residue at 600 ºC (%) of pure nanocellulose were 366 ºC and 21.4%. For the studies of the effect nanocellulose on polymer matrix, the results revealed that it was occured into two stages: (i) slightly increased from 270 to 276 ºC in the first stages and (ii) from 367 to 376 ºC second stages compared to pure PLLA-PEG-PLLA films as well as the residue of biocomposite films slightly increased (3.65-3.99%). The thermal stability increased with the content of nanocellulose due to the good interaction between the functional groups of nanocellulose and the polymer matrix [21].

TABLE-1
TGA ANALYSIS OF NANOCELLULOSE, MODIFIED NANOCELLULOSE, PLLA-PEG-PLLA/NC AND PLLA-PEG-PLLA/MODIFIED NANOCELLULOSE

Sample	$T_{d1,\ max}$ (°C)	$T_{d2,\ max}$ (°C)	Residue at 600 °C (%)
Nanocellulose	366	–	21.4
Pure film	270	367	1.43
1% Biocomposite film	269	368	3.65
3% Biocomposite film	274	372	3.67
5% Biocomposite film	276	376	3.99

The DSC curves of pure PLLA-PEG-PLLA film and PLLA-PEG-PLLA/NC biocomposite films are shown in Fig. 8. The glass transition (T_g), melting temperature (T_m) and cold crystallization (T_{cc}) peaks of the pure PLLA-PEG-PLLA films were 27 ºC, 165-170 ºC and 63-65 ºC, respectively. For PLLA-PEG-PLLA/NC composite film, it was found that T_g was slightly decreased (from 27 to 25 ºC) and T_{cc} (from 65 to 63 ºC), while T_m (from 168 to 167 ºC) was same due to weak interaction

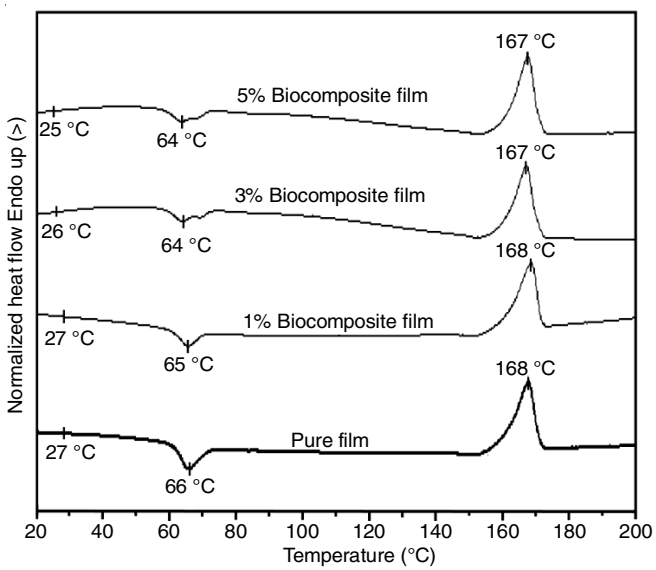

Fig. 8. DSC curves of pure PLLA-PEG-PLLA film, PLLA-PEG-PLLA/NC biocomposite films and pure nanocellulose

TABLE-2
THERMAL TRANSITION PROPERTIES OF PLLA-PEG-PLLA/NC AND PLLA-PEG-PLLA/MODIFIED NANOCELLULOSE COMPOSITE FILMS

Sample	Filler content (wt%)	T_g (°C)	T_m (°C)	T_{cc} (°C)	ΔH_m (J/g)	ΔH_{cc} (J/g)	X_c (%)
Pure film	0	27	168	65	42.410	13.260	37.5
1% Biocomposite film	1.0	26	168	65	39.795	7.246	42.3
3% Biocomposite film	3.0	25	167	63	41.986	6.851	46.6
5% Biocomposite film	5.0	25	167	63	44.271	7.618	49.6

and poor dispersion nanocellulose. The experimental results showed that the T_g of biocomposite films was slightly decreased. This can be attributed to the lower interactions of nanocellulose to change the mobility of polymer chains related to the glass transition. The T_m of the biocomposite film did not show a significant difference compared with that of pure PLLA-PEG-PLLA film. A reduction of T_{cc} indicates that the nanocellulose could enhance the crystallization process of the biocomposite films, acting as a nucleating agent [23,37].

The degree of crystallinity (X_c) of pure PLLA-PEG-PLLA film was observed at 37.4% (for DSC) and 4.28 % (from XRD) [7]. When nanocellulose (1-5% wt.) was added into the PLLA-PEG-PLLA matrix, it was observed that X_c increased from 37.4 to 49.6% from DSC (Table-2) and 4 to 19.2% from XRD. The increased X_c of biocomposite film according to nanocellulose content, indicating a nucleating effect induced by nanocellulose [23].

Conclusion

In this research, the extraction of cellulose from rice straw was successfully achieved. The particle size of cellulose had a diameter of 59.92 and 392 nm from particle size analysis and thus can be called nanocellulose. Different formulations of the nanocellulose and polymer matrix (PLLA-PEG-PLLA) at different ratios (1%, 3% and 5% wt.) were prepared using the solvent method. The thermal properties of the fabricated biocomposite films at 1%, 3% and 5% wt. displayed a slightly increased thermal stability in the first stages and second stages for TGA and slightly decreased T_g and T_{cc}, while T_m not different. Due to the interaction and good dispersion, it was found that Young's modulus slightly increased, stress at break and elongation at break of biocomposite films as compared to pure PLLA-PEG-PLLA film. It was found that the degree of crystallinity (X_c) of biocomposite film increased according to nanocellulose content, indicating the nucleating effect induced by nanocellulose. The results of this research showed that nanocellulose affects the polymer matrix by improved crystallinity and mechanical and thermal properties.

ACKNOWLEDGEMENTS

This research was financially supported by Thailand Research Fund (TRF). The Center of Excellence for Innovation in Chemistry (PERCH-CIC), Ministry of Higher Education, Science, Research and Innovation is gratefully acknowledged. The department of chemistry, Faculty of Science, Mahasarakham University

CONFLICT OF INTEREST

The authors declare that there is no conflict of interests regarding the publication of this article.

REFERENCES

1. A. Samir, F.H. Ashour, A.A.A. Hakim and M. Bassyouni, *npj Mater. Degrad.*, **6**, 68 (2022); https://doi.org/10.1038/s41529-022-00277-7
2. S.S. Panchal and D.V. Vasava, *ACS Omega*, **5**, 4370 (2020); https://doi.org/10.1021/acsomega.9b04422
3. R. Auras, B. Harte and S. Selke, *Macromol. Biosci.*, **4**, 835 (2004); https://doi.org/10.1002/mabi.200400043
4. Y. Ikada and H. Tsuji, *Macromol. Rapid Commun.*, **21**, 117 (2000); https://doi.org/10.1002/(SICI)1521-3927(20000201)21:3<117::AID-MARC117>3.0.CO;2-X
5. M.S. Singhvi, S.S. Zinjarde and D.V. Gokhale, *Appl. Mircobiol. Int.*, **127**, 1612 (2019); https://doi.org/10.1111/jam.14290
6. J. Ahmed and S.K. Varshney, *Int. J. Food Prop.*, **14**, 37 (2011); https://doi.org/10.1080/10942910903125284
7. Y. Baimark, W. Rungseesantivanon and N. Prakymoramas, *Mater. Des.*, **154**, 73 (2018); https://doi.org/10.1016/j.matdes.2018.05.028
8. Y. Hu, Y.S. Hu, V. Topolkaraev, A. Hiltner and E. Baer, *Polymer*, **44**, 5681 (2003); https://doi.org/10.1016/S0032-3861(03)00609-8
9. Y. Srisuwan and Y. Baimark, *Polymer*, **14**, 3186 (2022); https://doi.org/10.3390/polym14153186
10. R.M. Santos, W.P. Flauzino Neto, H.A. Silvério, D.F. Martins, N.O. Dantas and D. Pasquini, *Ind. Crops Prod.*, **50**, 707 (2013); https://doi.org/10.1016/j.indcrop.2013.08.049
11. P.J. Jandas, S. Mohanty and S.K. Nayak, *J. Clean. Prod.*, **52**, 392 (2013); https://doi.org/10.1016/j.jclepro.2013.03.033
12. A. Wang, R. Qi, C. Xiong and M. Huang, *Iran. Polym. J.*, **20**, 281 (2011).
13. S.C. Pech-Cohuo, G. Canche-Escamilla, A. Valadez-González, V.V.A. Fernández-Escamilla and J. Uribe-Calderon, *Int. J. Polym. Sci.*, **2018**, 3567901 (2018); https://doi.org/10.1155/2018/3567901
14. C.C.S. Coelho, M. Michelin, M.A. Cerqueira, C. Gonçalves, R.V. Tonon, L.M. Pastrana, O. Freitas-Silva, A.A. Vicente, L.M.C. Cabral and J.A. Teixeira, *Carbohydr. Polym.*, **192**, 327 (2018); https://doi.org/10.1016/j.carbpol.2018.03.023
15. A. Isogai, *J. Wood Sci.*, **59**, 449 (2013); https://doi.org/10.1007/s10086-013-1365-z
16. W.P. Flauzino Neto, H.A. Silvério, N.O. Dantas and D. Pasquini, *Ind. Crops Prod.*, **42**, 480 (2013); https://doi.org/10.1016/j.indcrop.2012.06.041
17. P. Lu and Y.-L. Hsieh, *Carbohydr. Polym.*, **87**, 564 (2012); https://doi.org/10.1016/j.carbpol.2011.08.022
18. M. Aminu, *Int. J. Nanomater. Nanotechnol. Nanomed.*, **3** 051 (2017); https://doi.org/10.17352/2455-3492.000021
19. M. Thakur, A. Sharma, V. Ahlawat, M. Bhattacharya and S. Goswami, *Mater. Sci. Energy Technol.*, **3**, 328 (2020); https://doi.org/10.1016/j.mset.2019.12.005
20. M.B. Agustin, B. Ahmmad, S.M.M. Alonzo and F.M. Patriana, *J. Reinf. Plast. Composit.*, **33**, 2205 (2014); https://doi.org/10.1177/0731684414558325
21. A.B. Perumal, P.S. Sellamuthu, R.B. Nambiar and E.R. Sadiku, *Appl. Surf. Sci.*, **449**, 591 (2018); https://doi.org/10.1016/j.apsusc.2018.01.022
22. P. Lu and Y.-L. Hsieh, *Carbohydr. Polym.*, **82**, 329 (2010); https://doi.org/10.1016/j.carbpol.2010.04.073

23. S.H. Sung, Y. Chang and J. Han, *Carbohydr. Polym.*, **169**, 495 (2018); https://doi.org/10.1016/j.carbpol.2017.04.037
24. D.P. Chattopadhyay and B.H. Patel, *J. Text. Sci. Eng.*, **06**, (2016); https://doi.org/10.4172/2165-8064.1000248
25. Y.H. Lim, I.M.L. Chew, T.S.Y. Choong, M.C. Tan and K.W. Tan, *MATEC Web Conf.*, **59**, 04002 (2016); https://doi.org/10.1051/matecconf/20165904002
26. E.S. Abdel-Halim, *Arabian J. Chem.*, **7**, 362 (2014); https://doi.org/10.1016/j.arabjc.2013.05.006
27. C. Zhang, L. Liao and S. Gong, *Macromol. Rapid Commun.*, **28**, 422 (2007); https://doi.org/10.1002/marc.200600709
28. H. Danafar, K. Rostamizadeh, S. Davaran and M. Hamidi, *Drug Dev. Ind. Pharm.*, **40**, 1411 (2014); https://doi.org/10.3109/03639045.2013.828223
29. L. Li, Z.Q. Cao, R.Y. Bao, B.H. Xie, M.B. Yang and W. Yang, *Eur. Polym. J.*, **97**, 272 (2017); https://doi.org/10.1016/j.eurpolymj.2017.10.025
30. L. Du, J. Wang, Y. Zhang, C. Qi, M.P. Wolcott and Z. Yu, *Nanomaterials*, **7**, 51 (2017); https://doi.org/10.3390/nano7030051
31. Z. Liu, M. He, G. Ma, G. Yang and J. Chen, *J. Korea Tech. Assoc. Pulp Pap. Ind.*, **51**, 40 (2019); https://doi.org/10.7584/JKTAPPI.2019.04.51.2.40
32. B. Nasri-Nasrabadi, T. Behzad and R. Bagheri, *J. Appl. Polym. Sci.*, **131**, 40063 (2014); https://doi.org/10.1002/app.40063
33. P. Jariyasakoolroj, N. Rojanaton and L. Jarupan, *Polym. Bull.*, **77**, 2309 (2020); https://doi.org/10.1007/s00289-019-02862-4
34. Z. Tang, C. Zhang, X. Liu and J. Zhu, *J. Appl. Polym. Sci.*, **125**, 1108 (2012); https://doi.org/10.1002/app.34799
35. R.Z. Khoo, H. Ismail and W.S. Chow, *Procedia Chem.*, **19**, 788 (2016); https://doi.org/10.1016/j.proche.2016.03.086
36. A. Alemdar and M. Sain, *Bioresour. Technol.*, **99**, 1664 (2008); https://doi.org/10.1016/j.biortech.2007.04.029
37. S. Fehri, P. Cinelli, M.-B. Coltelli, I. Anguillesi and A. Lazzeri, *Int. J. Chem. Eng. Appl.*, **7**, 85 (2016); https://doi.org/10.7763/IJCEA.2016.V7.548